JMEPEG (2010) 19:123–128
DOI: 10.1007/s11665-009-9414-x

©ASM International
1059-9495/$19.00

Relationship Between Embedding Depth and Residual Stress in the cBN Grain of Monolayer Brazed Abrasive Tools

W.F. Ding, J.H. Xu, Z.Z. Chen, Y.C. Fu, and H.H. Su

(Submitted July 21, 2008; in revised form February 16, 2009)

The relationship between the embedding depth and the residual stress in the brazed cBN grains is analyzed experimentally in order to optimize the embedding depth of grains in the monolayer brazed abrasive tools. It is found that the residual stress is stable without remarkable gradient in the core zones of the brazed grains. However, the stress distribution gradient is rather great in the regions such as both ends of the central axis, the margin region of the central plane in the cBN grains, and the margin region of the section plane between the grains and the filler top. The maximum tensile stress in the margin zone of the brazed cBN grains has the most important influence on the mechanical property of the grains. The embedding depth is accordingly optimized at 30-40% of the total height of cBN grain.

Keywords advanced characterization, brazing, cBN grain, embedding depth, residual stress

1. Introduction

The monolayer brazed cubic boron nitride (cBN) abrasive tools realize strong joining to abrasive grains by virtue of the chemical reaction among the partners at elevated temperatures (Ref 1, 2). As a result, the typical shortcoming of the traditional electroplated and sintered abrasive tools, such as the grains fallout during the heavy-load grinding process, is avoided (Ref 3). Brazed cBN tools have shown distinguished advantages in machining nickel superalloy and titanium alloy, etc. (Ref 4, 5). It is evident, however, that the performance of the brazed abrasive tools depends not only on the quality and size of the utilized cBN grains, but also on the embedding depth of the brazed grains in the joining layer. Here the embedding depth is the distance between the grain bottom and the filler top on the working surface of the abrasive tools. If the embedding depth of grains is too large, then the chip storage space is insufficient, and the machining performance of the brazed abrasive tools is imperfect. On the contrary, if the embedding depth is small, fracture and cracking may occur in the brazed cBN grains even though strong joining between the abrasive grains and the filler alloy is realized in the brazing process (Ref 6). At this time, serious wear and high tool cost restrict the wide commercial application of the brazed cBN abrasive tools.

For the reason mentioned above, it becomes rather difficult to determine the embedding depth of the grains in the filler layer during fabrication of brazed cBN abrasive tools. All the above factors need to take synthetically into account the following aspects: the joining strength, the chip storage space, and the mechanical properties. In particular, the difference in the thermal expansion coefficients among three partners of brazed abrasive tools, such as brittle cBN grains, ductile filler alloy, and tool substrate, results in large residual stresses. Consequently, the mechanical strength of the brazed cBN grains may be negatively impacted. So far, these vital problems have seldom been studied though previous literature has focused on the reaction mechanism of cBN grain and Ag-Cu-Ti filler alloy at elevated temperatures (Ref 7-9). In the investigation of this study, the residual stresses in the brazed cBN grains are measured and the corresponding distribution characteristics are analyzed. The embedding depth of cBN grains on the working surface of the brazed abrasive tools is accordingly optimized.

2. Experimental Procedure

2.1 Materials

In general, it is not easy to ensure the uniform shape of cBN grains. In this study, the grains with both the long and short axes of 250 μm were chosen. In particular, though the sharp edges and corners exist on the surface of CBN grains, it is reasonable to assume a globular shape for these grains. Consequently, the grains may be regarded as having an axial symmetric structure. At the same time, $(Ag_{72}Cu_{28})_{95}Ti_5$ alloy is utilized as the active filler, which is considered as the joining layer of the abrasive tools in the present investigation. The tool substrate of AISI 1045 steel is a column with a diameter of 15 mm and a height of 5 mm.

2.2 Specimen Preparation

Prior to brazing, the raw materials mentioned above were cleaned. The three-layer sandwich structure of tool substrate/

W.F. Ding, J.H. Xu, Z.Z. Chen, Y.C. Fu, and **H.H. Su**, College of Mechanical Engineering, Nanjing University of Aeronautics and Astronautics, Nanjing, China. Contact e-mail: dingwf2000@vip.163.com.

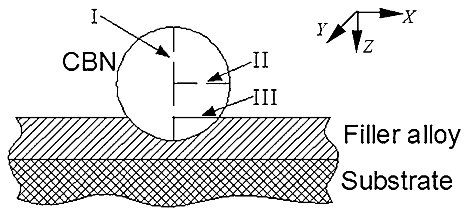

Fig. 1 Schematic showing the brazed CBN grain specimen

filler alloy/cBN grain was assembled, as presented in Fig. 1. The grain was placed by a fine pincer at the central point in the top layer of the filler alloy. Then the CBN grains were joined to the steel substrate via the chemical reaction at elevated temperatures in the brazing process. In this investigation, the embedding depth from 10 to 70% of the total grain height was controlled by adjusting the thickness of the filler layer. Brazing was performed in a vacuum furnace. The heating temperature and the dwell time were chosen as 920 °C and 5 min, respectively. These were the optimal processing parameters for brazing cBN grains, as described in Ref 10. Since the heating and cooling rate of 10 °C/min was rather low, the uniform temperature fields in the specimens were achieved during brazing. Accordingly, the residual stresses arising from the temperature variation of the joined partners may be very minimal and hence, neglected.

2.3 Residual Stress Measurement

Due to the sp^3 hybridization structure and small size of the CBN grain crystal, the conventional stress measurement techniques, such as strain resistance gauges and x-ray diffraction, were not able to measure the residual stresses in such limited regions as that of cBN grains. Recently, a method based on the complementary use of Fourier transform infrared (FTIR) spectroscopy has been developed for a quantitative evaluation of sp^2 and sp^3 bonded fraction in the BN crystal (Ref 11). Meanwhile, other stickies (Ref 12-16) have proposed to measure the stress distribution by means of detecting the deflection of the characteristic infrared (IR) absorption peak in stress-free cBN and the actual peak in stressed cBN. The peak shift of the cBN IR transverse optic (TO) absorption mode is expected to be simply proportional to the relative lattice compression, which has been proved valid for a cBN bulk crystal through the comparable experiments of the Raman and FTIR measurements under high hydrostatic pressure (Ref 17). Therefore, it is well justified to assume that the peak shift of the TO modes measured under isotropic pressure yields at least a first approximation of that found by FTIR at normal incidence. In this study, the measurement of FTIR spectrum of the brazed cBN grains was carried out along three directions. One is Line I in Fig. 1, that is, the central axis of the globular grain. Another is Line II, namely, the radial direction along X axis in the central plane parallel to the top layer of Ag-Cu-Ti filler alloy. The last is Line III in Fig. 1, that is, the radial direction along X axis in the section plane between the brazed cBN grain and the filler top. Among the three lines, Line I and Line II are the particular positions within the cBN grains, whereas Line III is always the margin region between the brazed grains and the filler layer. According to the distribution characteristics of the residual stress in brazed brittle materials, i.e., Si_3N_4, SiC, and Al_2O_3 ceramics, three special zones in Fig. 1 are always the potential regions where the maximum stress of the brazed grain perhaps exists. On the other hand, because of the supposed symmetric structure around the central axis, the stress fields are also regarded as symmetric. Therefore, the influence of the vector direction of the lines in Fig. 1 on the stress magnitude of the brazed cBN grains is neglected.

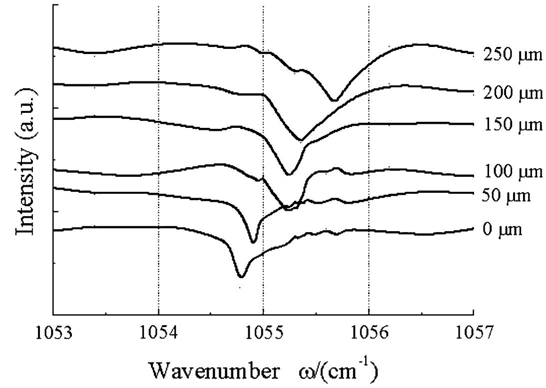

Fig. 2 Typical FTIR spectrum of brazed CBN grain

3. Results and Discussion

3.1 Distribution of the Residual Stress in the Central Axis of the Brazed cBN Grains

Figure 2 shows the typical FTIR spectrum curves in the central axis of a brazed cBN grain with 50% embedding depth. It is noted that the wavenumber of 1055 cm^{-1} is the characteristic peak position for cBN grain without stress (Ref 14, 15). Obviously, the absorption peaks display a certain excursion to the standard value of 1055 cm^{-1}. It implies that the brazed grain endures different residual stresses at the corresponding positions. Previous research has discovered that, the residual stress σ in cBN is given by (Ref 13):

$$\sigma = \frac{\Delta\varpi}{p} \qquad \text{(Eq 1)}$$

where $\Delta\varpi$ is the excursion value of the absorption peak and p is 4.5 cm^{-1}/GPa (Ref 14, 15).

According to Fig. 2 and Eq 1, the residual stresses in the central axis (Line I in Fig. 1) of the brazed cBN grains are achieved, as illustrated in Fig. 3. In general, the embedding depth has different influence on the stress distribution along Line I of the brazed cBN grain.

When the embedding depth is as small as 10-30% of the total, there exists a steady region with width of 75 μm within the top region of the brazed cBN grains. In this special region, the embedding depth does not affect the magnitude of the tensile stress that is below 40 MPa. However, significant fluctuation of the stress distribution occurs in the bottom region of the brazed grains. The reason is attributed to a strong interaction between cBN grain and Ag-Cu-Ti filler in the extremely narrow region such as the side and bottom surface of the brazed grains. Here, the interaction implies that the coordinating effect makes allowance for the difference in the thermal expansion coefficients at the joining interface of the cBN grains and Ag-Cu-Ti alloy.

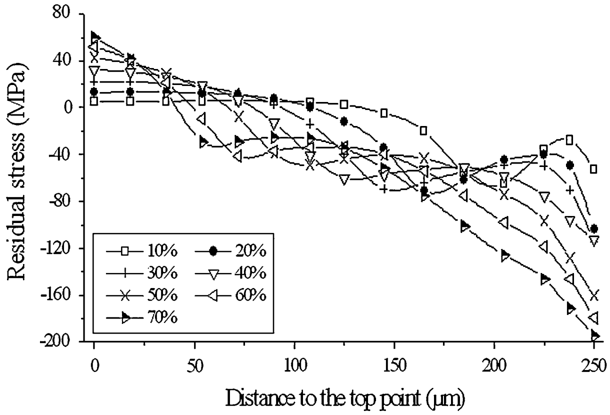

Fig. 3 The distribution of residual stress in the central axis of brazed CBN grains

When the embedding depth is above 40% of the brazed cBN grains, the fluctuation of the residual stress in the bottom region of Line I disappears, whereas significant distribution gradient of the residual stress is still observed. The maximum tensile stress is below 60 MPa. The deeper the embedding depth of grains, the greater the distribution gradient of the residual stress. In the bottom region of the brazed grains, the embedding depth shows a remarkable influence not only on the distribution gradient but also on the magnitude of the residual stress. The maximum compressive stress decreases with the decrease of the embedding depth. Figure 3 shows that the compressive stresses have reduced from 190 to 100 MPa for the embedding depths of 70 and 40%, respectively. Meanwhile, the distribution gradient is also quite distinct. On the other hand, in the middle region of the brazed cBN grains, the embedding depth has displayed significant influence not on the compressive stresses but on the width of the steady region of the residual stresses. For example, the width is about 30 μm for the embedding depth of 40% and approximately 100 μm for the depth of 60%.

3.2 Distribution of the Residual Stress in the Central Plane of the Brazed cBN Grains

Figure 4 demonstrates the residual stresses within the radial direction of the central plane (Line II in Fig. 1) in the brazed cBN grains. Though the stress magnitude and the width of the steady stress region change slightly in the core zone of the central plane, the stress gradient is very obvious in the margin region with the width of about 25 μm. Within Line II, when the embedding depth is below 50%, the margin regions of the brazed grains endure the tensile stress of 80 MPa. However, once the brazed grains are embedded surpassing the central plane, the residual stresses change from tensile to compressive. For instance, when the embedding depth attains 70% of the total height of cBN grain, the compressive stress increases up to 130 MPa.

If the grains are embedded shallowly, the tensile stresses along Line II increase gradually with increasing embedding depth. It can be seen from Fig. 4 that the tensile stress is only 5 MPa when the embedding depth is 10%, while the stress is increased to 80 MPa when the depth is increased to 30%. Meanwhile, though the residual stresses of the brazed cBN grains are almost uniform for the embedding depth of 10-20%, the stress gradient becomes remarkable when the embedding depth is above 30%.

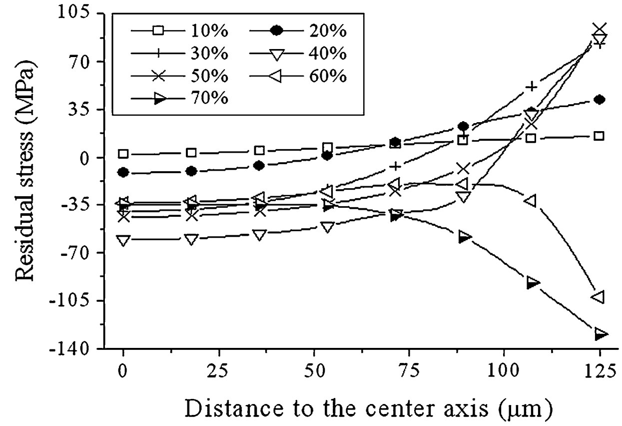

Fig. 4 The distribution of the residual stress in the central plane of brazed CBN grains

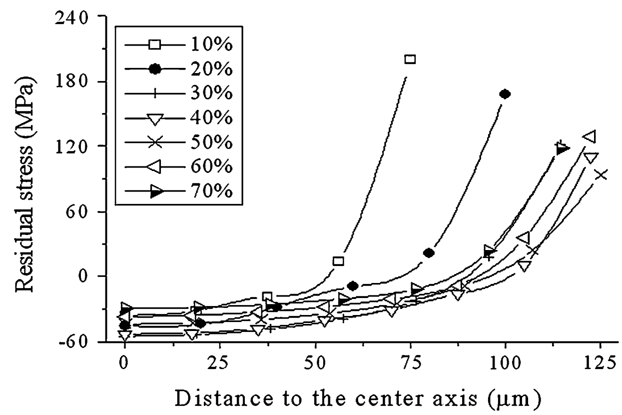

Fig. 5 The distribution of the residual stress in the section plane of brazed grains and filler alloy

3.3 Distribution of the Residual Stress in the Section Planes between the Brazed cBN Grains and the Filler Top

The stress distribution in the radial direction of the section planes (Line III in Fig. 1) between the brazed cBN grains and the top layer of filler alloy is illustrated in Fig. 5. As could be seen, when the grains are embedded deeply, no evident influence of the embedding depth exists on the residual stresses in the core region of the section planes. However, the stresses of the margin region within the section planes show a strong relationship with the embedding depth. The tensile stresses are about 90 MPa and 130 MPa for the embedding depth of 50 and 60%, respectively. Moreover, the distribution of the residual stresses also changes remarkably. When the embedding depth of the brazed grain is 40%, the compressive stress of 20 MPa in the core zone changes rapidly to the tensile stress of 110 MPa in the margin zone.

On the other hand, if the grain is embedded shallowly, the distribution gradient of the residual stresses is more obvious and the tensile stress becomes greater for the shallower embedding depth. When the embedding depth is 10%, the tensile stress reaches 200 MPa, as demonstrated in Fig. 5.

3.4 Mechanism of Stress Development in the Brazed cBN Grains

According to the analysis above, in the margin region of the section planes between the grains and the filler top, the grains

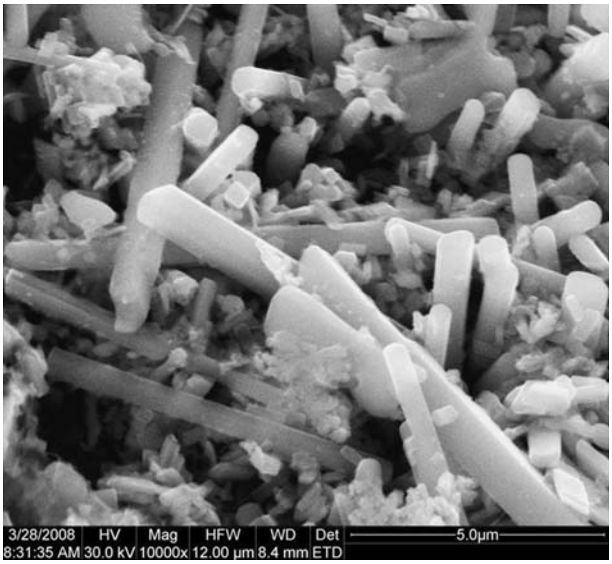

Fig. 6 Resultants formed at the brazing interface of CBN grain and Ag-Cu-Ti alloy

always endure the tensile stresses. The reason is that the margin region is a special interface, where the mechanical properties change drastically between brittle cBN abrasive grain and ductile Ag-Cu-Ti filler alloy. On the one hand, the brazing resultants, i.e., TiB_2, TiB, and TiN (Fig. 6), have a relaxation effect on the residual stress between the cBN grains and the filler alloy depending on the transitional interfacial microstructure of cBN/TiB_2/TiB/TiN/filler alloy (Ref 18). The difference between the thermal expansion coefficients is weakened to a certain extent. For example, the average thermal expansion coefficients of cBN, TiB_2, TiB, TiN, and Ag-Cu-Ti filler alloy over the temperature range of 20-800 °C are about 4.55×10^{-6}, 7.4×10^{-6}, 8.6×10^{-6}, 9.4×10^{-6}, and 20×10^{-6} K^{-1}, respectively. On the other hand, the compounds could not yet completely eliminate the residual stresses caused by the great difference in the mechanical property of the joined partners. Theoretically, the mechanical properties in the core zone of the brazed cBN grains are quite similar except for the existence the crystal defects of the grains. Under such circumstance, the trend is too weak to form the residual stresses because of the varied thermal expansion coefficients. The residual stresses are mainly controlled by the faint distortion of the crystal lattice in the inner zones of the grains, which is induced by the crystal distortion in the margin region of the section planes (Ref 15). Consequently, the residual stress is always low.

In addition, since the grain is a type of brittle material with high compressive strength and low tensile strength, the tensile stress has a vital influence on the mechanical strength of the brazed cBN grains (Ref 19, 20). If the tensile stress is too high in some inner region of the brazed grains, the special region is the dangerous one where the grain is likely to crack during the heavy-load grinding process or even during the brazing process because the strength of the brazed grains has been degraded. The service life and the machining performance of the brazed cBN abrasive tools are therefore decreased. Figure 7 provides the apparent evidence that when the embedding depth is 10%, a crack has been formed and expanded in the brazed cBN grain. It corresponds to the decreased grain strength due to the maximum tensile stress of 200 MPa.

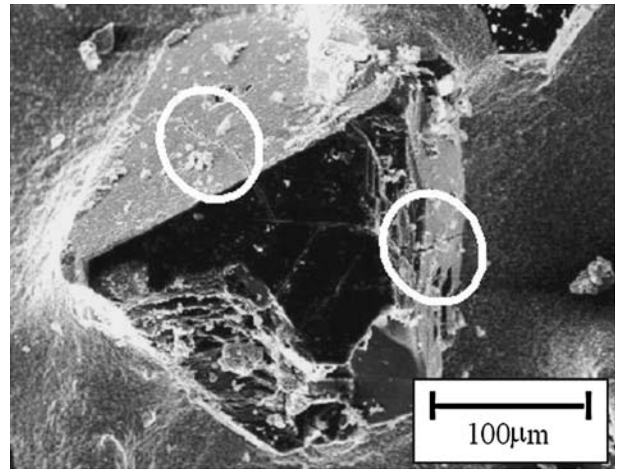

Fig. 7 Crack in the brazed CBN grain with embedding depth of 10%

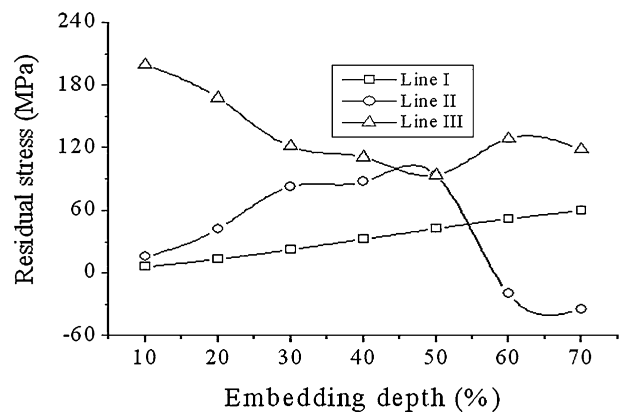

Fig. 8 Maximum residual stress in the special regions of brazed grain

3.5 Optimization of the Embedding Depth of the cBN Grains in the Monolayer Brazed Abrasive Tools

Just as described in the above analysis, the tensile stress is an important limiting factor to determine the mechanical strength of the brazed cBN grains. The embedding depth of the cBN grains in the filler layer has strong correlation with the maximum tensile stress. Consequently, it is reliable to optimize the embedding depth of the brazed grains based on the maximum tensile stress in the special zones as follows: the central axis, the radial direction in the central plane, and the radial direction in the section planes between cBN grain and filler top.

On the basis of Fig. 3-5, the influence of the embedding depth on the maximum stress along the three lines is exhibited in Fig. 8. As could be seen, the maximum tensile stress in the brazed grains does not change linearly with the embedding depth. When the embedding depth is below 30%, the maximum tensile stress decreases significantly with increasing embedding depth. However, when the embedding depth is above 30%, the maximum tensile stress does not vary markedly. It is attributed to the stress relaxation effect of the filler layer. As a result, the residual stresses are released via the ductile deformation of Ag-Cu-Ti filler alloy. Obviously, when the grains are embedded

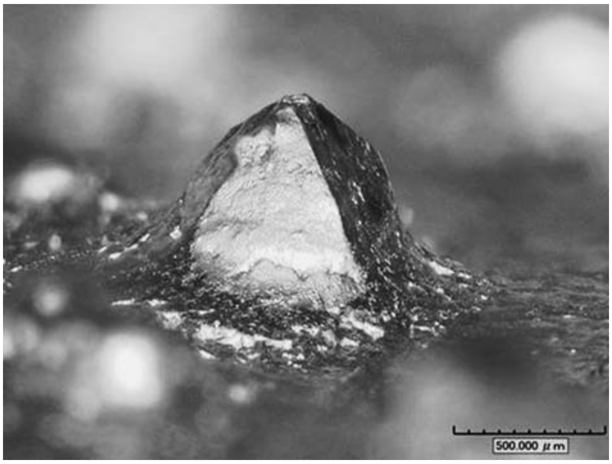

Fig. 9 The brazed CBN grain with embedding depth of 40%

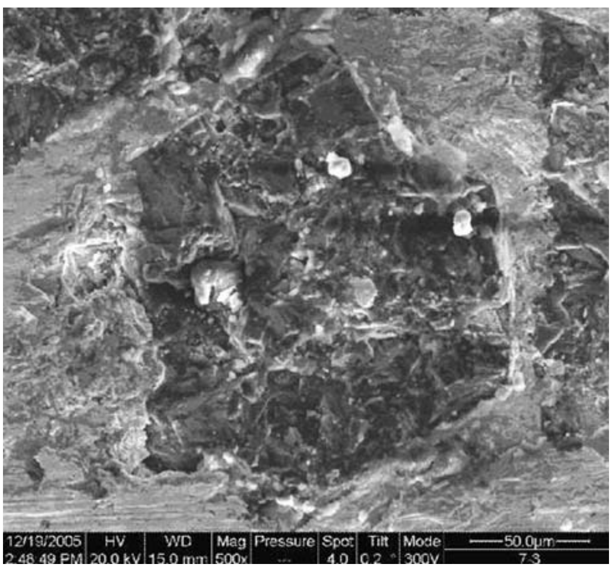

Fig. 10 Abrasion wear of the brazed CBN grains

between 30 and 70%, the maximum stresses of 100-120 MPa in the brazed cBN grains are lower than the stresses of the brazed grains with the embedding depth of 10-20%. Considering the chip storage space on the working surface of the brazed abrasive tools, the embedding depth is optimized at 30-40% of the whole grain. It is noted here that the applied grain embedding depth of the abrasive tools may be adjusted further according to the requirements of the machining process. Thus, not only the grain strength is ensured, but the essential chip storage space of tools is also obtained.

In this study, the grinding experiments of nickel superalloy have indicated that when the grains are embedded with 40% (Fig. 9). Abrasion wear is the primary wear form for the brazed cBN abrasive tools, as shown in Fig. 10. Cracking of CBN grains seldom takes place. Therefore, the brazed cBN abrasive tools with optimum grain embedding depth show better grinding performance and longer service life than the traditional electroplated and sintered counterparts.

4. Conclusions

The results are summarized as follows:

1. The residual stress is stable without remarkable gradient in the core zones of the brazed cBN grains. The variation of the stress distribution is rather significant in the three special zones such as both ends of the central axis, the margin regions of both the central planes, and the section planes.
2. Because of the tremendous difference in the thermal expansion coefficients of brittle cBN grain and ductile Ag-Cu-Ti filler alloy, the tensile stress always exist in the margin region of the section planes between the grains and the filler. Moreover, the stress gradient is large.
3. In order to ensure the grain strength and the essential chip storage space of the abrasive tools, the embedding depth is optimized at 30-40% of the whole grain according to the maximum tensile stress in the brazed cBN grains.

Acknowledgments

This research was financially supported by the National Basic Research Program of China (No. 2009CB724403), and Program for New Century Excellent Talents in University from Ministry of Education of China (No. NCET-07-0435).

References

1. A.K. Chattopadhyay and H.E. Hintermann, New Generation Superabrasive Tool with Monolayer Configuration, *Diam. Relat. Mater.*, 1992, **1**, p 1131–1143
2. G. Burkhard and F. Rehsteiner, High Efficiency Abrasive Tool for Honing, *Ann. CIRP*, 2002, **51**(1), p 271–274
3. J. Webster and M. Tricard, Innovation in Abrasive Products for Precision Grinding, *Ann. CIRP*, 2004, **53**(2), p 597–617
4. W.F. Ding, J.H. Xu, and J.B. Lu, Brazed CBN Grinding Wheel with Ag-base Filler Alloy, *Mater. Sci. Forum*, 2004, **471**, p 11–15
5. A. Ghosh and A.K. Chattopadhyay, Experimental Investigation on Performance of Touch-Dressed Single-Layer Brazed cBN Wheels, *Int. J. Mach. Tool Manuf.*, 2007, **47**(7–8), p 1206–1213
6. Y. Zhou, P.D. Funkenbusch, and D.J. Quesnel, Stress Distribution at the Abrasive-Matrix Interface During Tool Wear in Bound Abrasive Grinding—A Finite Element Analysis, *Wear*, 1997, **209**, p 247–254
7. M.G. Nicholas, D.A. Mortimer, and L.M. Jones, Some Observations on the Wetting and Bonding of Nitride Ceramics, *J. Mater. Sci.*, 1990, **25**, p 2679–2689
8. E. Faran, I. Gotman, and E.Y. Gutmanas, Experimental Study of the Reaction Zone at Boron Nitride Ceramic-Ti Metal Interface, *Mater. Sci. Eng.*, 2000, **288A**, p 66–74
9. X.Y. Ma, C.R. Li, and W.J. Zhang, Study on the Phase Diagram of the Ti-B-N System and the Interfacial Reaction of the Ti/BN Joints, *Mater. Sci. Eng.*, 2005, **392A**, p 394–402
10. W.F. Ding, J.H. Xu, and M. Shen, Development and Performance of Monolayer Brazed CBN Grinding Tools, *Int. J. Adv. Manuf. Technol.*, 2007, **34**(5–6), p 491–495
11. M.A. Djouadi, S. Ilias, and D. Bouchier, Quantitative Interpretation of Infrared Absorption Bands from Hexagonal, Cubic and Mixed Boron Nitride Films, *Diamond Relat. Mater.*, 1998, **7**, p 1657–1662
12. S. Ilias, V. Stambouli, D. Bouchier, and G. Nouet, Study of Stress and Infra-Red Absorption Line of BN Films Containing Various Fractions of Cubic Phase, *Diamond Relat. Mater.*, 2000, **9**, p 1867–1875
13. R.C. Fang, *Solid Spectroscopy*, University of Science and Technology of China, Hefei, 2001, p 355 (in Chinese)

14. A. Klett, R. Freudenstein, and M.F. Plass, Stress of c-BN Thin Films: A Parameter Investigation, *Surf. Coat. Technol.*, 1999, **116–119**, p 86–92
15. X.W. Zhang, Y.J. Zou, and H. Yan, Electrical Properties and Annealing Effects on the Stress of RF-Sputtered c-BN Films, *Mater. Lett.*, 2000, **45**, p 111–115
16. Y.N. Zhao, G.T. Zou, and B. Wang, Studies on the Stress in Cubic Boron Nitride Films by Infrared Spectroscopy, *Chem. J. Chin. Univ.*, 1998, **19**(7), p 1136–1139 (in Chinese)
17. J.A. Sanjurjo, E. Lopez-Cruz, P. Vogl, and M. Cardona, Dependence on Volume of the Phonon Frequencies and the IR Effective Charges of Several III-V Semiconductors, *Phys. Rev. B*, 1983, **28**, p 4579–4584
18. W.F. Ding, J.H. Xu, and Y.C. Fu, Delamination Behavior and Formation Mechanism of the Interfacial Microstructure in the Brazed Joint of Silver-Copper-Titanium Alloy and Cubic Boron Nitride Grain, *Chin. J. Mech. Eng.*, 2008, **44**(6), p 61–65 (in Chinese)
19. Z. Chen, Q.Z. Zhao, and F. Fang, Interfacial Reactions and Diffusion Path in Partial Transient Liquid-Phase Bonding of Si_3N_4/Ti/Ni/Ti/Si_3N_4, *Trans. Nonferr. Metal. Soc.*, 1999, **9**(4), p 831–837
20. B. Huang, Y.Q. Yang, and H.J. Luo, Effect of the Interfacial Reaction Layer Thickness on the Thermal Residual Stresses in SiC_f/Ti-6Al-4V Composites, *Mater. Sci. Eng.*, 2008, **489A**(1–2), p 178–186